Journal of Thermal Analysis, Vol. 37 (1991) 2525-2539

THERMODYNAMIC PROPERTIES OF AQUEOUS SOLUTIONS OF AMMONIUM NITRATE SALTS

C. S. Choi, J. Schroeder, Y. T. Lee, J. Frankel[+] and J. F. Cox[+]*

DEPARTMENT OF PHYSICS RENSSELAER POLYTECHNIC INSTITUTE TROY, NY 12180-3590
[+]U. S. ARMY RESEARCH AND DEVELOPMENT ENGINEERING CENTER AMCCOM, WATERVLIET ARSENAL, SMCAR-CCB-RP, WATERVLIET, NY 12189-4050 U.S.A.

(Received October 26, 1990; in revised form March 21, 1991)

We present Differential Scanning Calorimetry (DSC) results on Hydroxyl Ammonium Nitrate (HAN) solutions and Triethanol Ammonium Nitrate (TEAN) solutions with varying concentrations. These results are used to generate phase diagrams of these solutions. The results of the melting points of these liquids are compared with the theoretical calculations of the depression of melting points. The melting temperatures of the HAN solutions at some specified concentration range are predicted rather well using the two electrolyte assumption. The phase diagram of the TEAN solutions explains an instability with respect to phase separation of this liquid.

Aqueous solutions of Hydroxyl Ammonium Nitrate (HAN) and Triethanol Ammonium Nitrate (TEAN) are a particular type of liquid propellant which has long been recognized for their advantages due to large volumetric impetus and continuous varying charge possibilities. However, their accidental detonation causes major problems in both storage and handling [1, 2]. It is required that the liquid propellant remains a homogeneous liquid in the range from 328 K to 218 K [1]. Differential Scanning Calorimetry (DSC) is a powerful method for measuring possible storage reactions as a function of temperature. The main thermodynamic parameters which are needed for various intermolecular calculations are also provided by DSC. Whenever a material undergoes a change in its physical state, such as melting or phase transition,

* To whom all corespondence should be addressed

John Wiley & Sons, Limited, Chichester
Akadémiai Kiadó, Budapest

or whenever it reacts chemically, heat is absorbed or liberated. Many such processes can be initiated simply by raising the temperature of the material. Modern differential scanning calorimeters are designed to determine the melting points, latent heats, specific heats and enthalpies of this process by measuring the differential heat flow required to maintain a sample of the material and a reference at the same temperature. Also DSC has generally been used in determining the purity of the sample and its phase diagram.

Several years ago Fifer [3] carried out some DSC measurements to investigate the stability of HAN-based liquid propellants, the destabilizing effects of metal impurities, and the ignition temperatures in the temperature intervals from 600 K to 746 K. Also Lee *et al.* [4] explained the instability of this liquid by introducing the concept of the spinodal decomposition as determined by light scattering experiments. Here we present the results of DSC measurements at low temperatures with the emphasis on the phase transition, which can show the various low temperature characteristics of the liquid propellants. Since the liquid propellant is a ternary liquid, it is very important to study the physical and chemical characteristics of the two solutions (HAN and TEAN solutions) separately since binary solutions are more tractable to calculations.

Calculation of the melting temperature

The melting or freezing point of a pure compound is the temperature at which solid crystals of the substance are in an equilibrium condition with the liquid phase at atmospheric pressure. For solid substances which melt without decomposition, the melting point has a most important physical property. The melting point depression of an impure material can be calculated the from Clausius-Clapeyron equation [5],

$$\frac{\mathrm{d} \ln (p_A / p_o)}{\mathrm{d}T} = \frac{\Delta H}{RT^2}, \tag{1}$$

where p_A is a partial pressure of the pure component A, p_o is a partial vapor pressure of the pure component A at the same temperature, ΔH is a molar heat of fusion, R is the gas constant, and T is the equilibrium temperature in degrees Kelvin, respectively. Generally the molar heat of fusion, ΔH, is temperature dependent and given by,

$$\Delta H = \Delta H_o + \Delta C_p(T\text{-}T_m), \tag{2}$$

where ΔC_p is a difference of the molar heat capacity of the pure component for the liquid and solid phase, and T_m is a melting temperature. The partial vapor pressure, or the activity, of each component is, as defined by Raoult's law, proportional to its mole fraction, that is

$$p = N_A p_o,$$

where N_A is a mole fraction of A. Then one has

$$\ln\frac{p_A}{p_o} = \ln a_A = \ln N_A = \frac{-\Delta H_o}{R}\left(\frac{1}{T}-\frac{1}{T_m}\right) - \frac{\Delta C_p}{R}\left(1-\frac{T_m}{T}+\ln\frac{T_m}{T}\right), \quad (3)$$

where a_A is the activity coefficient of component A.

If the solution is a strong electrolyte, then the activity coefficient of the electrolyte in its aqueous solution, 'a', is given by [6]

$$a = \left(\frac{n}{r_w + n}\right)^n, \quad (4)$$

and r_w is defined by;

$$r_w = \frac{N_w}{1 - N_w} \quad (5)$$

where N_w is the mole fraction of water and n is the number of ions per molecule of salt. Therefore, the depression of the melting point of an aqueous solution with electrolytes is larger than that of a non-electrolyte solution.

Experimental aspects

All experiments were run on a Perkin Elmer DSC-4 equipped with a microprocessor controller, a digital interface, and a computer operating with thermal analysis software. The samples used are TEAN solutions, HAN solutions and mixtures of HAN and TEAN solutions (LP-1845 [7] plus additional water; LP-1845 plus additional HAN; and LP-1845 plus additional TEAN). The samples were made using a 13.34 molar HAN solution supplied by the US Army Ballistic Research Laboratory, TEAN crystals (Morton Thiokol, Inc., Lot No. 190), and distilled water. Impurities were removed by passing the sample through a 0.22 μm fretted filter, but there still exists the possibility

Table 1 Composition of samples

Sample No.	HAN		TEAN		WATER	
	Wt.%	Mole %	Wt.%	Mole %	Wt.%	Mole %
LP-1845	62.29	37.1	19.61	5.3	18.10	57.6
I-1	67.14	39.4	17.76	3.9	18.10	56.7
I-2	57.27	34.7	24.63	6.7	18.10	58.5
I-3	52.30	32.2	29.60	8.3	18.10	59.5
II-1	62.31	33.3	15.61	3.8	22.08	62.9
II-2	62.68	37.4	19.72	5.3	18.00	57.3
II-3	62.28	37.4	21.60	6.2	16.12	54.4
II-4	62.29	42.0	23.60	7.2	14.11	51.8
III-1	60.36	34.2	19.54	5.0	20.10	60.8
III-2	58.40	31.3	19.50	4.8	22.10	63.7
III-3	56.43	29.1	19.49	4.6	24.08	66.3
III-4	54.24	26.1	19.65	4.3	27.09	69.6
III-5	50.34	22.9	19.56	4.0	30.01	73.0
IV-1	49.8	21.1	15.7	2.9	34.5	76.0
IV-2	46.1	18.0	14.5	2.5	39.4	80.0
IV-3	38.9	13.0	12.3	1.8	48.8	85.0
IV-4	31.1	8.8	9.8	1.3	59.1	90.0
IV-5	17.8	4.3	5.6	0.6	76.4	95.0
IV-6	100.4	2.2	3.7	0.4	85.9	97.0
HW-1	83.71	49.1			16.29	50.9
HW-2	80.00	42.8			20.00	57.2
HW-3	77.61	39.4			22.39	60.6
HW-4	74.99	36.0			25.01	64.0
HW-5	69.24	29.7			30.76	70.3
HW-6	65.06	25.9			34.94	74.1
HW-7	60.00	22.0			40.00	78.0
HW-8	50.00	16.0			50.0	84.0
HW-9	30.00	7.4			70.0	92.6
HW-10	10.00	2.0			90.0	98.0
TW-1			79.00	24.2	21.00	75.8
TW-2			74.94	20.2	25.06	79.8
TW-3			69.72	16.4	30.28	83.6
TW-4			64.89	13.6	35.11	86.4
TW-5			60.24	11.4	39.76	88.6
TW-6			55.03	9.4	44.97	90.6
TW-7			50.28	7.9	49.72	92.1
TW-8			40.00	5.4	60.00	94.6
TW-9			20.00	2.1	80.00	97.9
TW-10			10.00	0.9	90.00	99.1

of introducing some impurities into the sample from the DSC pans. The list of samples is hown in Table 1 in which LP-I, LP-II, and LP-III are a series of samples whose water, HAN, and TEAN weight percents are the same as those of LP-1845, respectively; LP-IV is a series of samples of LP-1845 plus additional water (25 wt% to 500 wt% more water); TW means just TEAN plus water; and HAN plus water is HW.

The method for encapsulation of samples most widely adopted is the use of an aluminum pan with a domed lid which is crimped in position. Since there is some evidence that the liquid may react with the aluminum or metal ions, such as Cu^{+2} and Fe^{+3}, a more stable gold pan was substituted [3]. The average weight of gold pans was 131.80 ±1.60 mg and a typical weight of each sample was 5 mg. Nitrogen through a fine filter, needle valve, and flowmeter was used as a purge gas in the DSC. Generally both heating and cooling processes were run at a rate of 10 degree per minute. But different heating and cooling rates were used to see the effects of heating and cooling rates on the melting temperatures and the supercooling effects. A single crystal sapphire was used as a reference to calculate the heat capacities.

Results and discussion

Melting points of TEAN solutions

The melting points of all samples in Table 1 were measured. Since the lowest temperature our system could reach was 205 K, some samples did not show any phase changes. Every sample was measured both in a heating and cooling process. Our first attempt was to obtain the phase diagrams for our solutions by measuring the melting points. The phase diagrams of many binary aqueous electrolyte solutions have eutectic points or show melting hydrates, which can be divided into congruent, incongruent and semi- congruent melting [8]. If the compound has a congruent melting point, then both the liquid and the solid phase have the same composition.

Table 2 and Figs 1–2 show the results of the melting point measurements for the TEAN solutions. There were two peaks in many cases, even though for some compositions one peak is very broad and weak as shown in Fig. 1. In some samples (TW-5, 6, 7) it is hard to discriminate between the two peaks because they are so close together. As the concentration of water increases, the second peak becomes larger both in the heating and cooling process as shown in Fig. 1. However, there is no doubt these two peaks clearly indicate

the occurrence of a melting process. These two peaks can be explained if there is a recrystallization during melting or pre-melting [9, 10]. If this is the case, then the second peak may be changed considerably with different heating or cooling rates. After several measurements at heating rates of 20 to 1 deg per minute, we found that the second peaks did not change significantly. The onset melting temperature at a low heating rate is 2.2 degrees higher than that of the highest heating rate, and the enthalpy changes were almost

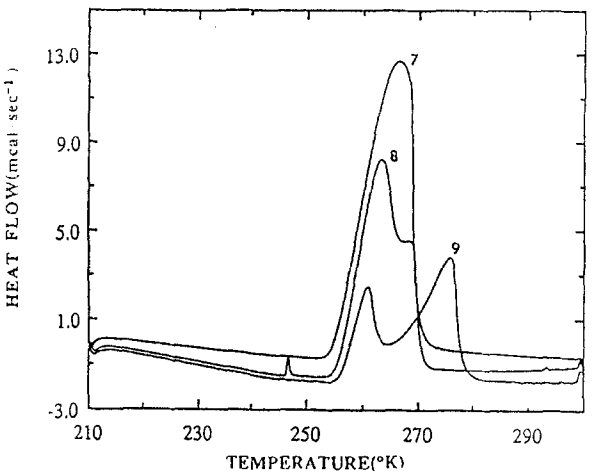

Fig. 1 Heating curves of TW-7, 8 and 9 at a heating rate of 10 degrees per minute. The lower temperature peaks designate the eutectic peaks

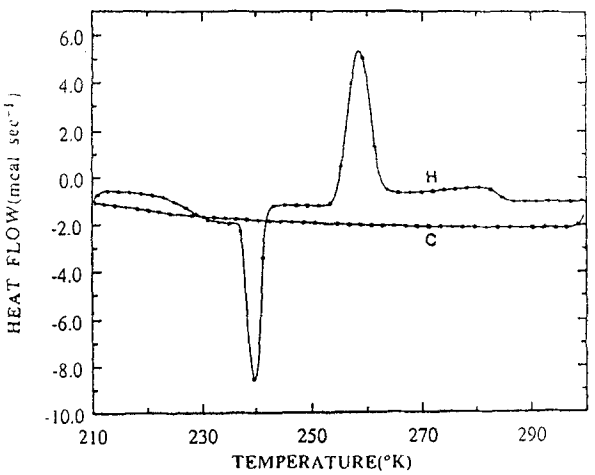

Fig. 2 Supercooling effects on TW-2. In the cooling process with a cooling rate of one degree per minute there is no peak, which shows a supercooling effect

constant within experimental error. Therefore, we think recrystallization is not a reason for these two endothermic peaks, but the low temperature exothermic peak may be attributed to the crystallization of the eutectic phases, because the low temperature peaks occur always at the same temperature regardless of the composition of the TEAN solution.

Table 2 Lower melting (eutectic) points of the TEAN solutions

Sample	Heating		Cooling	
	Peak K	Onset K	Peak K	Onset K
TW-1	259.5	255.9	241.3	242.2
TW-2	260.4	254.9	*No Peak	
TW-3	260.1	255.2	211.5	219.4
TW-4	257.0	255.4	235.0	243.0
TW-5	262.8	255.9	235.7	237.8
TW-6	262.3	255.6	239.9	241.7
TW-7	261.9	256.3	233.5	241.0
TW-8	263.5	256.8	238.6	245.7
TW-9	261.9	257.7	239.2	246.0
TW-10	260.1	258.0	*No Peak	

*TW-2 did not show any peak at all with various cooling rates and in the TW-10 case there was only one peak in the cooling process which was not believed as an eutectic peak.

All TEAN solutions show supercooling effects, especially TW-2 which shows no peak at all with various cooling rates of 1 to 20 deg per minute as shown in Fig. 2. Even though there is no exothermic peak in the cooling process for TW-2, the endothermic peaks were observed in every heating process at various heating rates. We found that there exists an exothermic peak before the onset of the endothermic peak in the heating process, which indicates that in a supercooled state the liquid behaves as if in a glassy state which has a very long relaxation time. During heating this supercooled liquid starts to crystalize at first and then it begins to melt at the melting temperature. It is rather clear from Table 2 and Fig. 1 that all the second peaks in the water-rich samples come from the free water, but the origin of the second peaks of the TEAN-rich samples is not that obvious. The second peak of TW-2 for the heating process was very repeatable but that of TW-1 was not.

The temperature differences between two peaks decrease as their water concentrations increased until they reach the eutectic composition, at which there is no temperature difference between the two. Our results show that the

eutectic composition of TEAN is between the composition of TW-5 and that of TW-7. Eutectic means 'easily soluable', so the solutions of TW-5, 6 and 7, whose mole fraction of TEAN is about 0.1 or the weight percent of TEAN is about 55 to 60%, are very homogeneous or the composition of the crystal and that of liquid are the same. Bogdanov and Mihailov [11, 12] explained the tendency for supercooling in the eutectic system as the formation of stable liquid water-crystal complexes and the necessity for their components to be separated during their eutectic crystallization. If this is true, then we can expect another eutectic point at the composition of TW-2 from its great supercooling tendency, but this is not obvious with the present data.

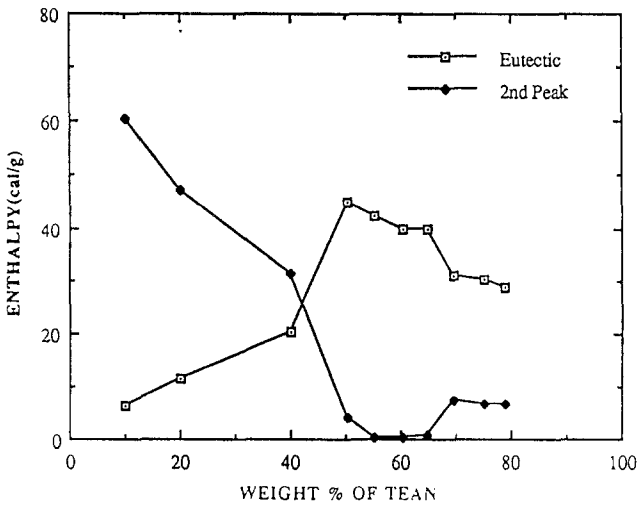

Fig. 3 Eutectic peak enthalpy and the enthalpy of the second peak (higher temperature peak) for the heating process as a function of weight percent of TEAN

The values at the eutectic peak in Table 2 and Fig. 3 give additional evidence for the eutectic composition of the TEAN solution, that is, the eutectic peaks of TW-5, 6 and 7 (weight % of TEAN is 55 to 60) are large and the enthalpy changes due to melting (higher temperature peaks) are small. Except for the eutectic composition, the enthalpy change is almost linear with respect to the weight percent of TEAN. To obtain a phase diagram of the TEAN solution, we measured the melting temperatures of the TEAN crystals and distilled water, and the onset melting temperatures were 354 K and 274 K, respectively.

As shown in Table 2 and 3, the melting temperatures are different from one another according to not only onset or peak temperatures but also with respect to each process (heating or cooling), therefore it is hard to say which temperature represents the real melting temperature. Because the onset temperatures seem to be more reliable than their peak values, the onset temperatures on the heating process are used as the melting temperatures to obtain a phase diagram of the TEAN solutions. Figure 4 shows the phase diagram of the TEAN solutions, in which we can see the eutectic composition being near the composition of TW-6. Below 250 K all TEAN solutions will be solidified and there exist liquid and solid phases together within the temperatures between two peaks except for the eutectic composition. The TEAN solutions will be very homogeneous at temperatures above the higher melting temperature, which depends on the composition of the solution.

Table 3 Higher melting points of TEAN solutions

Sample	Heating		Cooling	
	Peak K	Onset K	Peak K	Onset K
TW-1	289.0	271.1	239.0	–
TW-2	284.9	269.3	–	–
TW-3	275.0	268.0	–	–
TW-4	267.0	*	240.0	–
TW-5	264.0	*	236.0	–
TW-6	263.0	*	–	–
TW-7	263.0	*	239.0	240.3
TW-8	270.0	*	251.0	252.4
TW-9	278.0	269.0	256.9	258.5
TW-10	282.0	268.0	255.1	258.1

*Onset temperatures of TW-4 to 8 on the heating process are almost the same with peak temperatures.

Since we have measured the heats of fusion and melting temperatures of water and TEAN crystals, we can calculate the theoretical melting temperature depression for the aqueous solution of TEAN by using Eqs (3), (4) and (5). The heat of fusion of TEAN was 6665 calories per mole and that of water was 1434 calories per mole and the difference of the heat capacities between the solid and liquid phases were from 150 to 400 mcal per gram per degree. Figure 4 shows the comparison between theoretical and experimental results of the phase diagram of the TEAN solutions with the two electrolyte assump-

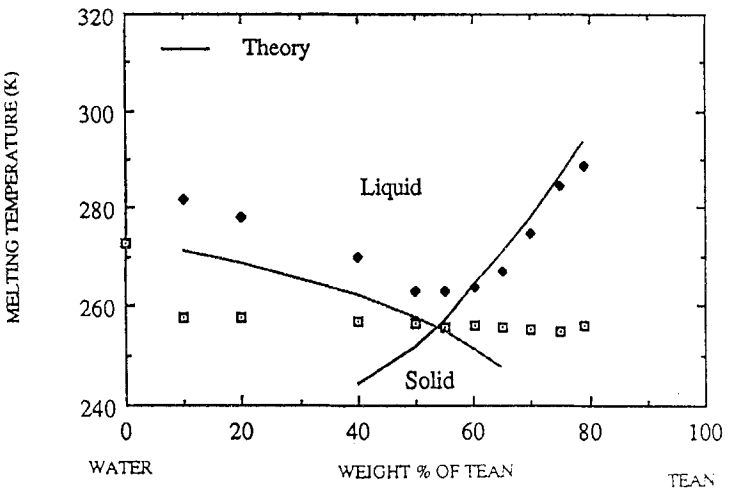

Fig. 4 Comparisons of measured melting temperatures of TEAN solutions and theoretical expectations with the two electrolyte assumptions. Here, ◆ and ⊡ are measured values of the melting temperatures where the higher melting point and the eutectic point were employed, respectively.

tions in the TEAN solutions. Here it is very clear that the theoretical and experimental eutectic compositions are almost the same even though there is a five degree difference in the eutectic temperatures.

Melting points of the HAN solutions

Melting temperatures of the HAn solutions are displayed in Table 4. Both the heating and cooling processes did not show any endothermic or exothermic peaks at all for the HW-1 to 4 samples. Some DSC results for the HAN solutions are shown in Fig. 5. There are endothermic and exothermic peaks in the heating and cooling processes for HW-5 to 10, but the peaks during heating are always much broader than those during cooling so large errors appear in determining the onset temperatures and in calculating the enthalpy changes for the HAN solutions during heating. These endothermic peaks become sharper as the concentration of HAN decreses, as seen in Fig. 5. We believe that this broadening comes from the change in solubility of HAN due to temperature changes. Every DSC result for the HAN solution shows only one peak over the entire temperature range, which means there is no eutectic peak for this solution. Consequently, the HAN solution is always homogeneous and the compositions of the crystal and liquid phases are the same for this temperature range. It is known that the 93 weight percent HAN

Table 4 Melting point of HAN solutions. The differences of the peak temperatures between the heating and cooling process is about 20 degrees without regard to the concentrations of TEAN

Sample	Heating		Cooling	
	Peak K	Onset K	Peak K	Onset K
TW-5	229.0	–	208.0	–
TW-6	–	223.6	212.0	237.0
TW-7	243.2	230.5	220.8	222.4
TW-8	253.8	242.6	232.7	233.8
TW-9	266.4	255.4	247.2	248.0
TW-10	276.3	265.4	253.5	255.0

solution has both liquid and solid phases at room temperature [13]. From this we believe there exists a possibility to have the eutectic point below 215 K. The melting points for the heating and cooling processes are very close together and the differences are almost the same without any evidence for a dependence on the concentration of HAN as shown in Table 4 and Fig. 6.

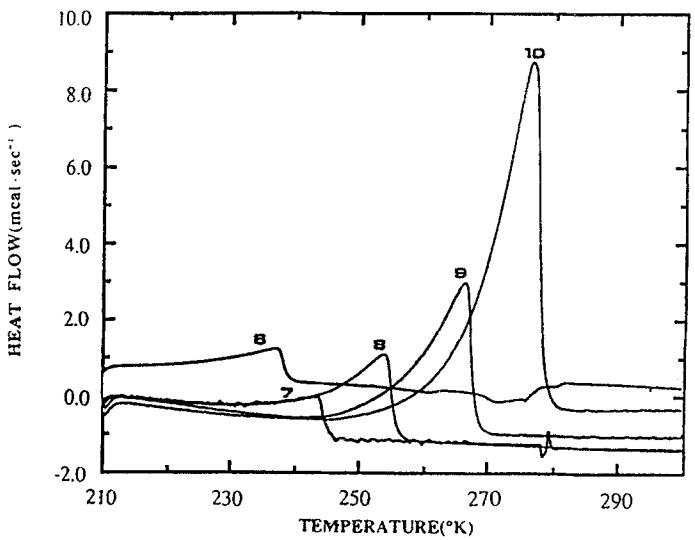

Fig. 5 DSC results of HW-6, 7, 8, 9, and 10 with a heating rate of 10 degrees per minute

This confirms that there is a much smaller supercooling effect for the HAN solution than for the TEAN solution. The extent of supercooling is strongly dependent on the degree of homogeneity of the solution, consequently, the

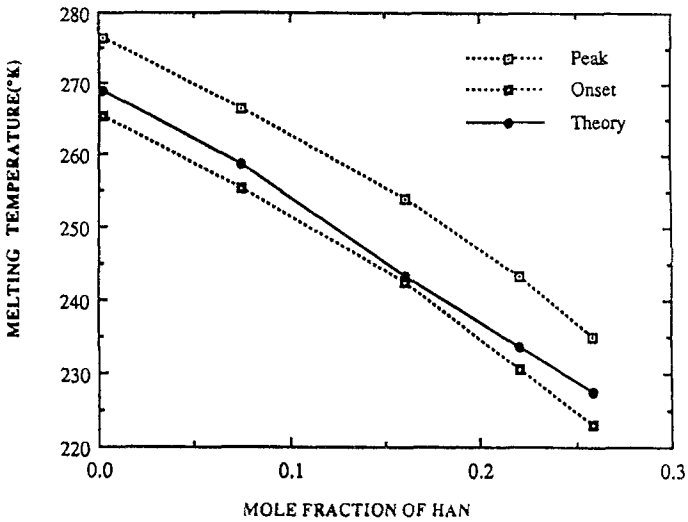

Fig. 6 Comparison between measured and calculated melting temperatures for the HAN solution

absence of supercooling is very consistent with the absence of an eutectic peak. The calculated melting temperatures of HAN solutions from Eqs (3), (4) and (5) with the two electrolyte assumption are in good agreement with the measured melting temperatures as shown in Fig. 6.

HAN solution plus TEAN solution

We have done some DSC measurements on LP-1845 plus additional water, HAN, and TEAN, but with the exception of some samples with relatively large amounts of water, no meaningful exothermic and endothermic peaks were observed in the temperature range of interest. As pointed out by Fifer [3], some DCS peaks of small amplitude were not repeatable. Attempts were made to observe effects on the heat capacity at constant pressure, due to a variation in the HAN and TEAN concentration, but no effects were observed. It is evident that the weight percent of water is a very important factor in governing the melting phenomena. As shown in Fig. 7, the melting temperature is almost linear with respect to the mole fraction of water. With a simple assumption that the melting temperature of the liquid is proportional to the mole fraction of water we can estimate the melting temperature of LP-1845. The result is consistent with the expected melting temperature from the

measurment of viscosity as a function of temperature and pressure [13] and also the results of Knapton [14].

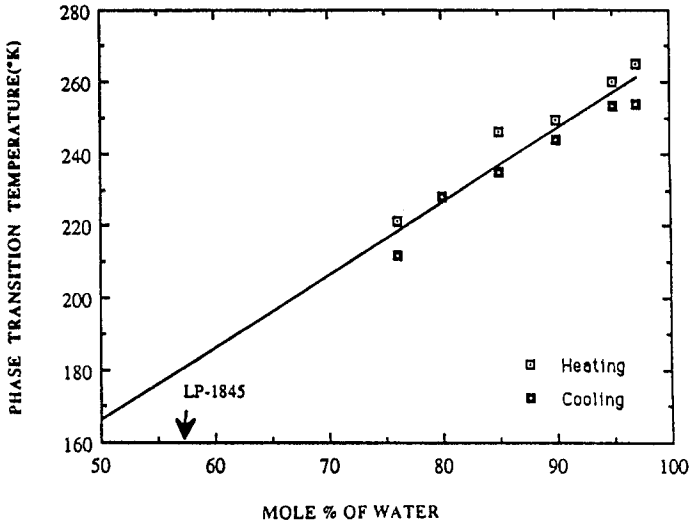

Fig. 7 Phase transition temperatures of LP-1845 with additional water

Conclusions

Using DSC techniques, the phase diagrams of TEAN and HAN were determined. The phase diagram for the TEAN solutions shows the eutectic point at 55 to 60 weight % of TEAN at about 260 K. Below the eutectic temperature, the TEAN solution solidified for all compositions except for the eutectic composition. The TEAN solutions have two endothermic peaks, one of which is the eutectic peak. So between these two temperatures, both the solid phase and liquid phase co-exist but the composition of these two phases will be different, which may manifest itself by phase separation effects [4,15,16]. Also we observed this phase separation through a long time storage test, and this may be responsible for an instability in LP-1845. The expected melting temperatures by theory agree with measured melting temperatures for the TEAN solutions with the two electrolyte assumptions, which also lead to almost the same eutectic composition. The TEAN solutions have a great tendency toward supecooling, and it seems to depend on the concentration of TEAN. The HAN solutions however, exhibit a smaller supercooling effect which seems not to be concentration dependent. The HAN solutions did not show any autectic point within our temperature range. The measured melting

temperatures of the HAN solutions are linearly dependent on the mole fraction of HAN, but we could not obtain any melting temperatures of HAN solutions with mole fractions of HAN larger than 0.3. But an eutectic point below 215 K is expected and it can be predicted if the heat of fusion of pure HAN is available.

The co-existence curve was estimated by measuring melting temperatures of LP-1845 plus additional water with the simple assumption that the phase transition temperature is approximately proportional to the mole fraction of water. The results we obtained through DSC measurements are quite consistent with the results from our shear viscosity measurement and also to the observed melting temperature by Knapton [14].

* * *

This work was supported in part by U.S. Army under ARO contract DAAA22-85-C-0218. We also wish to acknowledge many helpful discussions with N. Klein and J. D. Knapton of Ballistic Research Laboratory, Aberdeen Proving Ground, Aberdeen, MD, USA.

References

1 N. Klein, Proc. 19th JANNAF Combustion Meeting. Vol. I, CPIA Publ. 366, Laurel, MD, 1982.
2 C. A. Van Dijk and R. G. Priest, Combustion and Flame, 57 (1984) 15.
3 R. A. Fifer, L. J. Decker and P. J. Duff, Proc. 22nd JANNAF Combustion Meeting, Vol. II, Oct., 1985, p. 203.
4 Y.-T. Lee, J. Schroeder, C. S. Choi and J. Frankel, J. Chem. Phys., 92 (1990) 3283.
5 For example, F. Reif, Fundamentals of statistical and thermal physics, McGraw-Hill, Inc., New York 1965, p. 304.
6 J. H. Hildebrand, Solubility, Am. Chem. Soc. Monograph Series, The Chemical Catalog Company, Inc., New York, 1924, p. 165.
7 W. O. Seals and N. Swynnerton, Chemical analysis of liquid propellant, 1986 JANNAF Propulsion Meeting, Vol. I, New Orleans, Aug., 1986. The composition of LP-1845 in Table 1 is different from the nominal composition, which is water 16.8%, HAN 63.3% and TEAM 20.8%.
8 E. L. Skau and C. Arthur, Jr., Physical methods of chemistry A. Weissberger, Ed., New York, Wiley-Interscience, 1971, p. 105.
9 L. Mandelkern and A. L. Allou, Jr., J. Polymer Sci., B4 (1966) 447.
10 L. Mandelkern, J. G. Faton, R. Denison and J. Justin, J. Polymer Sci., B3 (1965) 803.
11 B. Bogdanov and M. Mihailov, J. Polym. Sci., Polym. Phys., 23 (1985) 2149.
12 B. Bogdanov and M. Mihailov, J. Thermal Anal. 30 (1985) 1027.
13 C. S. Choi, J. Schroeder and Y.-T. Lee, submitted to J. Chem. Phys.
14 J. D. Knapton and W. F. Morrison, Low temperature properties of HAN based propellants, US Army Ballistic Research Laboratory, 1984.
15 J. Schroeder, Treatise on Material Science and Technology; GlassI: Interaction with Electromagnetic Fields, Ed. M. Tomozawa and R. H. Doremus, Academic, New York 1977, p. 157.
16 S. Y. Hsich, R.W.Gammon, P. B. Macedo and C. J. Montrose, J. Chem. Phys., 56 (1972) 1663.

Zusammenfassung — Es werden DSC-Untersuchungen an Hydroxylammoniumnitrat- (HAN) und Triethanolammoniumnitrat- (TEAN) Lösungen unterschiedlicher Konzentration dargestellt. Anhand der Ergebnisse wurden Phasendiagramme für diese Lösungen erstellt. Die gemessenen Schmelzpunkte dieser Flüssigkeiten wurden mit den theoretischen Berechnungen der Schmelzpunkterniedrigung verglichen. Die Schmelztemperaturen der HAN-Lösungen in einem bestimmten Konzentrationsbereich können viel besser unter Zuhilfenahme der Zwei-Elektrolyten-Annahme abgeschätzt werden. Das Phasendiagramm der TEAN-Lösungen belegt eine Instabilität in Übereinstimmung mit einer Phasenseparierung in dieser Flüssigkeit.